

Dynamical Analysis of modified Reissner Nordström metric in lyra's geometry

Swarnabha Debnath¹, Dr. Biswajit Paul², Dr. Subrata Bhowmik³

¹Shiv Nadar University, Physics Undergraduate, Greater Noida, Delhi NCR, UP, PIN 201314

²Assistant Professor at Department of Physics, National Institute Of Technology Agartala, West Tripura, PIN 799046

³Associate Professor at Department of Mathematics, Tripura University, Agartala, West Tripura, PIN 799022

DOI: <https://doi.org/10.5281/zenodo.8131008>

Published Date: 10-July-2023

Abstract: We have applied the principles of Lyra's geometry in modifying the Reissner Nordström metric to develop the metric for charged black holes and derived the first two components of the metric from the modified Einstein's field equation. In this paper we analysed the complex dynamical system for the trajectories of the charged particles in the context of lyra's geometry based on Sen and Dunn's modification of the coupled Einstein-maxwell equation. The analysis begins by formulating the modified geodesic equations of motion for the RN metric in Lyra's geometry. As a result some interesting properties of the interaction of charged particles with the Reissner blackhole are studied.

Keywords: Dynamical analysis, Modified Reissner Nordström metric, Lyra's geometry, Scalar field, Phase space analysis, Stability analysis, Bifurcations, Scalar potential, Coupling constants.

1. INTRODUCTION

Lyra geometry extends the classical Riemannian geometry by introducing an extra geometric structure called a gauge field. It is equipped with metric tensor, which measures the distance and angles between the points similar to Riemannian geometry. However it also incorporates a gauge field, which is a vector field associated with the manifold. The gauge field introduces additional degrees of freedom and effects the geometric properties of the manifold. The generalised lyra's metric can be written in the format of Reissner metric for a spherically symmetric system [2],

$$ds^2 = e^\lambda dt^2 - e^\nu dr^2 - r^2 d\theta^2 - r^2 \sin^2 \theta d\phi^2 \quad (1.2)$$

Sen and Dunn and W.D.Halford [1] proposed a modification to the Einstein field equations by incorporating a scalar tensor theory of gravity which was named as Lyra's scalar field,

$$R_{\mu\nu} - \frac{1}{2} g_{\mu\nu} R + \frac{3}{2} \phi_\mu \phi_\nu - \frac{3}{4} g_{\mu\nu} \phi_k \phi^k = -x T_{\mu\nu} \quad (2.2)$$

Here, represent the Lyra's scalar field, which introduces an additional contribution to the curvature of spacetime. Lyra's scalar potential is a concept in theoretical physics that extends Einstein's theory of general relativity. It introduces an extra scalar field into the theory, which allows for the incorporation of a preferred direction or a background gauge field.

The generalised Reissner metric cited from the works of Jonatan Nordebo[6] and Ramesh Tikekar[7], is compared with the Lyra's metric to determine the unknown parameters, drawing inspiration from the works of W.D. Halford [1] and F. Rahaman, A. Ghosh, and M. Kalam[2]. By considering the Lyra's field equations and assuming exponential terms for the electromagnetic and gravitational potentials (e^λ and e^ν , respectively), expressions for these terms are derived. This leads to the derivation of the modified metric for the Reissner Nordström solution in Lyra's geometry, as explored in the works of R.R. Cuzinatto, E.M. de Morais, B.M. Pimentel paper of LyST[5] and D.K. Sen[1]. To study the dynamics of charged particles in this modified system, the geodesic equations governing their motion are derived as described by R.R. Cuzinatto, E.M. de Morais, and B.M.[3]. Pimentel and D.K. Sen papers for geodesics[4]. The analysis further explores the effects of

varying conditions on the gravitational and electromagnetic potentials, particularly focusing on the behaviour of the coupling constant with changing distance parameter r.

2. MODIFIED REISSNER NORDSTRÖM METRIC

The generalised Reissner Nordström metric [6] and [7],

$$ds^2 = B(r)c^2 dt^2 - A(r)dr^2 - r^2 d\theta^2 - r^2 \sin^2 \theta d\phi^2 \quad (2.1)$$

Otherhand the lyra's metric [2],

$$ds^2 = e^\lambda dt^2 - e^\nu dr^2 - r^2 d\theta^2 - r^2 \sin^2 \theta d\phi^2 \quad (2.2)$$

Comparing both the equations, we will replace B(r) as e^λ and A(r) as e^ν later in our calculations.

We will consider the conditions for the Reissner metric:

$$\Lambda = 0$$

$$g_{\mu\nu} = \begin{bmatrix} B(r)c^2 & 0 & 0 & 0 \\ 0 & -A(r) & 0 & 0 \\ 0 & 0 & -r^2 & 0 \\ 0 & 0 & 0 & -r^2 \sin^2 \theta \end{bmatrix}$$

$$T_{\mu\nu} = \frac{1}{\mu_0} \left[F_{\alpha\mu} F^{\alpha\beta} g_{\nu\beta} - \frac{1}{4} g_{\mu\nu} F^{\alpha\beta} F_{\alpha\beta} \right]$$

$$A_0 = \frac{Q}{4\pi\epsilon_0 r}, A_i = 0$$

$$\text{And, } g^{\mu\nu} = \begin{bmatrix} \frac{1}{B(r)c^2} & 0 & 0 & 0 \\ 0 & \frac{-1}{A(r)c^2} & 0 & 0 \\ 0 & 0 & \frac{-1}{r^2} & 0 \\ 0 & 0 & 0 & \frac{-1}{r^2 \sin^2 \theta} \end{bmatrix}$$

For Christoffel's symbols we will use, $\Gamma_{\mu\nu}^\rho = \frac{1}{2} g^{\rho\sigma} (\partial_\mu g_{\nu\sigma} + \partial_\nu g_{\mu\sigma} - \partial_\sigma g_{\mu\nu})$

$$\Gamma_{13}^3 = \Gamma_{31}^3 = \frac{1}{r}$$

$$\Gamma_{11}^1 = \frac{A'}{2A}$$

$$\Gamma_{33}^2 = -\sin \theta \cos \theta$$

$$\Gamma_{12}^2 = \Gamma_{21}^2 = \frac{1}{r}$$

$$\Gamma_{22}^1 = \frac{-r}{A}$$

$$\Gamma_{10}^0 = \Gamma_{01}^0 = \frac{B'}{2B}$$

$$\Gamma_{23}^3 = \Gamma_{32}^3 = \cot \theta$$

$$\Gamma_{00}^1 = \frac{c^2 B'}{2A}$$

$$\Gamma_{33}^1 = \frac{-r \sin^2 \theta}{A}$$

Therefore we place the values of these christoffel's symbols to get the ricci tensors as follows;

$$R_{00} = c^2 \left[\frac{-B''}{2A} + \frac{B'}{4A} \left(\frac{A'}{A} + \frac{B'}{B} \right) - \frac{B'}{rA} \right] \quad (2.3)$$

$$R_{11} = \frac{B''}{2B} - \frac{B'}{4B} \left(\frac{A'}{A} + \frac{B'}{B} \right) - \frac{A'}{rA} \quad (2.4)$$

$$R_{22} = -1 - \frac{r}{2A} \left(\frac{A'}{A} - \frac{B'}{B} \right) + \frac{1}{A} \quad (2.5)$$

$$R_{33} = \sin^2 \theta \left[-1 - \frac{r}{2A} \left(\frac{A'}{A} - \frac{B'}{B} \right) + \frac{1}{A} \right] \quad (2.6)$$

Now putting B as e^λ and A as e^ν to get the following terms, $A' = \nu' e^\nu$, $B' = \lambda' e^\lambda$, $B'' = \lambda'^2 e^\lambda + e^\lambda \lambda''$ and the following metric,

$$R_{\mu\nu} = \begin{bmatrix} \frac{-(\lambda'^2 e^\lambda + e^\lambda \lambda'')}{2e^\nu} + \frac{\nu' \lambda' e^\lambda}{4e^\nu} + \frac{\lambda'^2 e^\lambda}{4e^\nu} - \frac{\lambda' e^\lambda}{r e^\nu} & 0 & 0 & 0 \\ 0 & \frac{\lambda'^2 + \lambda''}{2} - \frac{\lambda'}{4} (\lambda' + \nu') - \frac{\nu'}{r} & 0 & 0 \\ 0 & 0 & -1 - \frac{r}{2e^\nu} (\nu' - \lambda') + \frac{1}{e^\nu} & 0 \\ 0 & 0 & 0 & \sin^2 \theta \left(-1 - \frac{r}{2e^\nu} (\nu' - \lambda') + \frac{1}{e^\nu} \right) \end{bmatrix}$$

2.1 Simplifying lyra's field from least action:

Lyra's field as described in [1] $R_{\mu\nu} - \frac{1}{2} g_{\mu\nu} R + \frac{3}{2} \phi_\mu \phi_\nu - \frac{3}{4} g_{\mu\nu} \phi_k \phi^k = -x T_{\mu\nu}$ is modified in context of the Reissner Nordström field by considering the least action for lyra's field as given in D.K.Sen's paper [8],

$$S = S_m + S_\phi \quad (2.1.1)$$

$$s = \int [\sqrt{-g}(R - 2\Lambda + \mathcal{L}_m) + \lambda(\phi_i \phi_i - \alpha^2)] d^4x, \quad (2.1.2)$$

where α is the constant parameter and λ is the lagrange multiplier, $\phi_i \phi_i$ is the sum of squares of components of scalar field ϕ and $\lambda(\phi_i \phi_i - \alpha^2)$ signifies a constraint on the scalar field ϕ and $(R - 2\Lambda + \mathcal{L}_m)$ is G_{ij} and $\lambda(\phi_i \phi_i - \alpha^2)$ is T_{ij} .

By considering $\frac{\partial s}{\partial g_{ij}} = 0$, we get,

$$\sqrt{-g} G_{ij} + \lambda T_{ij} = 0 \quad (2.1.3)$$

$$G_{ij} = R_{ij} - \frac{1}{2} R g_{ij} \quad (2.1.4)$$

From (2.1.3),

$$G_{ij} = -8\pi G T_{ij} + \lambda T_{ij} - 2\lambda \phi_i \phi_j + 2\lambda \delta_{ij} \phi_i \phi_j \quad (2.1.5)$$

Using (2.1.4) we can rewrite as,

$$R_{ij} - \frac{1}{2} R g_{ij} = -8\pi G T_{ij} + \lambda T_{ij} - 2\lambda \phi_i \phi_j + 2\lambda \delta_{ij} \phi_i \phi_j \quad (2.1.6)$$

Now by putting G_{ij} as $(R - 2\Lambda + \mathcal{L}_m)$ and T_{ij} as $\lambda(\phi_i \phi_i - \alpha^2)$ and a bit more simplification

$$R_{ij} - \frac{1}{2} R g_{ij} + \frac{3}{2} \lambda (\phi_i \phi_j - \alpha^2) - \frac{3}{4} \lambda \phi_r \phi^r g_{ij} = -8\pi G T_{ij} \quad (2.1.7)$$

Considering (2.1.7) in the context of lyra's field we get and changing the indices to μ and ν .

$$R_{\mu\nu} - \frac{1}{2} R g_{\mu\nu} + \frac{3}{2} \phi_\mu \phi_\nu - \frac{3}{4} \phi_k \phi^k g_{\mu\nu} = -k T_{\mu\nu} \quad (2.1.8)$$

Simplifying (2.1.8) based on the initial scalar conditions given $R=0$ when $\Lambda = 0$,

$$R_{\mu\nu} = k T_{\mu\nu} + \frac{3}{2} \phi_\mu \phi_\nu - \frac{3}{4} \phi_k \phi_k \quad (2.1.9)$$

2.2 Modified Field Equations:

The Faraday's tensor using $F_{\mu\nu} = \partial_\mu A_\nu - \partial_\nu A_\mu$ and initial conditions $A_0 = \frac{Q}{4\pi\epsilon_0 r}$, $A_i = 0$,

$$F^{\mu\nu} = \begin{bmatrix} 0 & \frac{-Q}{4\pi\epsilon_0 r^2 AB} & 0 & 0 \\ \frac{Q}{4\pi\epsilon_0 r^2 AB} & 0 & 0 & 0 \\ 0 & 0 & 0 & 0 \\ 0 & 0 & 0 & 0 \end{bmatrix}$$

$$\text{And, } F^{\alpha\beta} F_{\alpha\beta} = F^{01} F_{01} + F^{10} F_{10} = \frac{-Q^2}{8\pi^2 \epsilon_0^2 r^4 AB} \quad (2.2.1)$$

Using (2.2.1) in $T_{\mu\nu} = \frac{1}{\mu_0} [F_{\alpha\mu} F^{\alpha\beta} g_{\nu\beta} - \frac{1}{4} g_{\mu\nu} F^{\alpha\beta} F_{\alpha\beta}]$ we get,

$$T^{\mu\nu} = \begin{bmatrix} \frac{-Q^2}{32\mu_0\pi^2\epsilon_0^2r^4A} & 0 & 0 & 0 \\ 0 & \frac{Q^2}{32\mu_0\pi^2\epsilon_0^2r^4B} & 0 & 0 \\ 0 & 0 & \frac{-Q^2}{32\mu_0\pi^2\epsilon_0^2r^2AB} & 0 \\ 0 & 0 & 0 & \frac{-\sin^2\theta Q^2}{32\mu_0\pi^2\epsilon_0^2r^2AB} \end{bmatrix}$$

For deriving the Lyra's field equations we will take the reference from Sen and Dunn's proposal [2] by power function law,

Let, $\phi = ar^n$, by modifying as given in [2],

$\phi = \sum_{n=0}^{\infty} a_n r^{-n}$, where r is the radius of metric and a_n depends on coupling between gravity and electromagnetism.

As per our assumptions, i) No vacuum energy ii) Charged point singularity iii) Static, spherically symmetric, the components of each of the scalar potentials are;

$$\phi_0(n=0) = a_0, \quad (2.2.2)$$

$$\phi_1(n=1) = \frac{a_1}{r}, \quad (2.2.3)$$

$$\phi_2(n=2) = 0, [a_2 \ll r^2] \quad (2.2.4)$$

$$\phi_3(n=3) = 0, [a_3 \ll r^3] \quad (2.2.5)$$

Therefore, $= [a_0 + \frac{a_1}{r}]$; where a₀ and a₁ are very smaller than r.

$$\begin{aligned} \text{And, } \frac{3}{4} \phi_k \phi_k &= \frac{3}{4} \left[\sum_{n=0}^{i=3} \frac{a_n}{r^n} \right]^2 \\ &= \frac{3}{4} \left(a_0 + \frac{a_1}{r} \right)^2 \\ &= \frac{3}{4} a_0^2 + \frac{3 a_0 a_1}{2 r} \end{aligned}$$

Therefore the modified field equations using (2.1.9) are;

$$\frac{-(\lambda'^2 e^{\lambda+e\lambda\lambda'})}{2e^{\nu}} + \frac{\nu'\lambda'e^{\lambda}}{4e^{\nu}} + \frac{\lambda'^2 e^{\lambda}}{4e^{\nu}} - \frac{\lambda'e^{\lambda}}{re^{\nu}} = k \left(\frac{-Q^2}{32\mu_0\pi^2\epsilon_0^2r^4e^{\nu}} \right) + \frac{3}{4} a_0^2 - \frac{3 a_0 a_1}{2 r} \quad (2.2.6)$$

$$\frac{\lambda'^2 + \lambda''}{2} - \frac{\lambda'}{4} (\lambda' + \nu') - \frac{\nu'}{r} = k \left(\frac{-Q^2}{32\mu_0\pi^2\epsilon_0^2r^4e^{\lambda}} \right) - \frac{3}{4} a_0^2 - \frac{3 a_0 a_1}{2 r} \quad (2.2.7)$$

$$-1 - \frac{r}{2e^{\nu}} (\nu' - \lambda') + \frac{1}{e^{\nu}} = k \left(\frac{-Q^2}{32\mu_0\pi^2\epsilon_0^2r^2e^{\nu}e^{\lambda}} \right) - \frac{3}{4} a_0^2 - \frac{3 a_0 a_1}{2 r} \quad (2.2.8)$$

$$\sin^2 \theta \left(-1 - \frac{r}{2e^{\nu}} (\nu' - \lambda') + \frac{1}{e^{\nu}} \right) = k \left(\frac{-\sin^2 \theta Q^2}{32\mu_0\pi^2\epsilon_0^2r^2e^{\nu}e^{\lambda}} \right) - \frac{3}{4} a_0^2 - \frac{3 a_0 a_1}{2 r} \quad (2.2.9)$$

2.3 Computing e^{λ} and e^{ν} :

Dividing (2.2.6) by e^{λ} and dividing (2.2.7) by e^{ν} we get;

$$\frac{-(\lambda'^2 + \lambda'')}{2e^{\nu}} + \frac{\nu'\lambda'}{4e^{\nu}} + \frac{\lambda'^2}{4e^{\nu}} - \frac{\lambda'}{re^{\nu}} = k \left(\frac{-Q^2}{32\mu_0\pi^2\epsilon_0^2r^4e^{\nu}e^{\lambda}} \right) + \frac{3 a_0^2}{4 e^{\lambda}} - \frac{3 a_0 a_1}{2 r e^{\lambda}} \quad (2.3.1)$$

$$\frac{\lambda'^2 + \lambda''}{2e^{\nu}} - \frac{\lambda'}{4e^{\nu}} (\lambda' + \nu') - \frac{\nu'}{re^{\nu}} = k \left(\frac{Q^2}{32\mu_0\pi^2\epsilon_0^2r^4e^{\lambda}e^{\nu}} \right) - \frac{3 a_0^2}{4 e^{\nu}} - \frac{3 a_0 a_1}{2 r e^{\nu}} \quad (2.3.2)$$

Adding (2.3.1) and (2.3.2);

$$\frac{-\lambda'}{r e^{\nu}} - \frac{\nu'}{r e^{\nu}} = \frac{3}{4} a_0^2 \left(\frac{-1}{e^{\nu}} + \frac{1}{e^{\lambda}} \right) - \frac{3}{2} \frac{a_0 a_1}{r} \left(\frac{1}{e^{\lambda}} + \frac{1}{e^{\nu}} \right) \quad (2.3.3)$$

After simplifying (2.3.3) we get;

$$\frac{e^{\lambda}}{e^{\nu}} = \frac{\left(\frac{3}{4} a_0^2 - \frac{3 a_0 a_1}{2 r} \right)}{\left(-\frac{\lambda' + \nu'}{r} + \frac{3}{4} a_0^2 + \frac{3 a_0 a_1}{2 r} \right)} \quad (2.3.4)$$

By simplifying (2.3.2) we can write;

$$e^{\lambda} = \frac{k Q^2}{32 \mu_0 \pi^2 \epsilon_0^2 r^4 \left(\frac{\lambda'^2 + \lambda''}{2} - \frac{(\lambda'^2 + \lambda' \nu')}{4} - \frac{\nu'}{r} + \frac{3}{4} a_0^2 + \frac{3 a_0 a_1}{2 r} \right)} \quad (2.3.5)$$

From (2.3.4);

$$e^{\nu} = \frac{\left(-\frac{\lambda' + \nu'}{r} + \frac{3}{4} a_0^2 + \frac{3 a_0 a_1}{2 r} \right) e^{\lambda}}{\left(\frac{3}{4} a_0^2 - \frac{3 a_0 a_1}{2 r} \right)} \quad (2.3.6)$$

Using (2.3.5),

$$e^{\nu} = \frac{\left(-\frac{\lambda' + \nu'}{r} + \frac{3}{4} a_0^2 + \frac{3 a_0 a_1}{2 r} \right) k Q^2}{\left(\frac{3}{4} a_0^2 - \frac{3 a_0 a_1}{2 r} \right) (32 \mu_0 \pi^2 \epsilon_0^2 r^4) \left(\frac{\lambda'^2 + \lambda''}{2} - \frac{(\lambda'^2 + \lambda' \nu')}{4} - \frac{\nu'}{r} + \frac{3}{4} a_0^2 + \frac{3 a_0 a_1}{2 r} \right)} \quad (2.3.7)$$

Let, the constant a_0 and a_1 in equation (2.2.2) and (2.2.3) related to the gravitational potential and electromagnetic force respectively considered in respect to the lyra's blackhole system. Therefore;

$$a_0 = k_0 M \quad (2.3.8)$$

where k_0 represents a dimensionless constant and this expression contributes to the mass term.

And,
$$a_1 = k_1 \left(\frac{Q}{R} \right)^2 \quad (2.3.9)$$

where k_1 is a dimensionless constant relating to the electromagnetic term.

In Lyra's geometry gauge field can be a combination of both a vector field and a scalar field, in regarding to the lyst paper[5], it's given that $\lambda(r) = A_{\mu} = \phi_k^{-1} \partial_{\mu} \ln \phi_k^2$; but it's given initially that $A_0 = \frac{Q}{4\pi\epsilon_0 r}$, $A_{\mu} = 0$. Therefore $\lambda(r)$ will be the vector potential;

$$\lambda(r) = A_{\mu} = A_0 = \frac{Q}{4\pi\epsilon_0 r} \quad (2.3.10)$$

$$\frac{\partial \lambda}{\partial t} = 0, \frac{\partial \lambda}{\partial \phi} = 0, \frac{\partial \lambda}{\partial \theta} = 0$$

Also,
$$\frac{\partial \lambda}{\partial r} = \frac{-Q}{4\pi\epsilon_0 r^2}, \frac{\partial^2 \lambda}{\partial r^2} = 0$$

And, the scalar potential $v(r)$ is also related to the gauge potential ϕ as;

$$v(r) = V_{\mu} = \alpha \phi \quad (2.3.11)$$

where, α is the coupling constant.

$$\frac{\partial v}{\partial t} = \alpha \frac{\partial \phi}{\partial t} = 0 \quad [\text{as } \phi = \sum_{n=0}^{\infty} a_n r^{-n}]$$

$$\frac{\partial v}{\partial r} = \alpha \frac{\partial \sum_{n=0}^{\infty} a_n r^{-n}}{\partial r}$$

$$= \alpha \left[\frac{\partial \left(\frac{a_1}{r} \right)}{\partial r} \right]$$

$$= \alpha \frac{-a_1}{r^2} = 0 \quad (\text{as } a_1 \ll r^2)$$

And, $\frac{\partial^2 v}{\partial r^2} = 0, \frac{\partial v}{\partial \theta} = 0, \frac{\partial v}{\partial \phi} = 0.$

Using (2.3.10) and (2.3.11) and their derivatives we can simplify (2.3.5) and (2.3.7);

$$e^\lambda = \frac{kQ^2}{32\mu_0\pi^2 \epsilon_0^2 r^4 \left(\frac{3}{4}a_0^2 + \frac{3a_0 a_1}{2r}\right)} \tag{2.3.12}$$

$$e^\nu = \frac{kQ^2}{\left(\frac{3}{4}a_0^2 - \frac{3a_0 a_1}{2r}\right)(32\mu_0\pi^2 \epsilon_0^2 r^4)} \tag{2.3.13}$$

By replacing the values of e^λ and e^ν the modified Reissner Nordström metric in lyra’s geometry is as follows;

$$ds^2 = \frac{kQ^2}{32\mu_0\pi^2 \epsilon_0^2 r^4 \left(\frac{3}{4}a_0^2 + \frac{3a_0 a_1}{2r}\right)} dt^2 - \frac{kQ^2}{\left(\frac{3}{4}a_0^2 - \frac{3a_0 a_1}{2r}\right)(32\mu_0\pi^2 \epsilon_0^2 r^4)} dr^2 - r^2 d\theta^2 - r \sin^2 \theta d\phi^2 \tag{2.3.14}$$

where, $a_0 = k_0 M$ and $a_1 = k_1 \left(\frac{Q}{R}\right)^2$, a_0 and a_1 are very smaller than r .

Here, a_0 incorporate the mass of blackhole into lyra’s potential and k_0 adjusts the relative strength of mass contribution.

And, a_1 influence the electric charge on lyra’s potential and reflects the expected behaviour of the electric field of the blackhole which diminishes with the radial distance r^2 and k_1 adjust the relative strength of charge contribution.

3. GEODESIC EQUATIONS FOR THE MODIFIED REISSNER NORDSTRÖM METRIC:

Using the general geodesic equation,

$$\ddot{x}^i = \sum_{j=0}^3 \sum_{k=0}^3 \Gamma_{jk}^i \dot{x}^j \dot{x}^k + qF^{ik} \dot{x}^k \tag{3.1}$$

where θ, t, r have the derivatives with respect to a affine parameter τ and as Reissner blackholes are spherically symmetric in theory, so all the components of derivatives of ϕ will vanish and therefore the geodesics are;

$$\dot{z} = \frac{-yz}{r} \tag{3.2}$$

$$\dot{y} = \frac{Q}{8\pi\epsilon_0 r^2} \left(\frac{\frac{3}{4}k_0^2 M^2 - \frac{3k_0 k_1 M \left(\frac{Q}{R}\right)^2}{r}}{\frac{3}{4}k_0^2 M^2 + \frac{3k_0 k_1 M \left(\frac{Q}{R}\right)^2}{r}} \right) x^2 + \frac{qQ(32\mu_0\pi^2 \epsilon_0^2 r^4)^2}{4\pi\epsilon_0 r^2 (kQ^2)^2} \left[\left(\frac{3}{4}k_0^2 M^2\right)^2 - \left(\frac{3k_0 k_1 M \left(\frac{Q}{R}\right)^2}{r}\right)^2 \right] x + \frac{r}{(kQ^2)} (32\mu_0\pi^2 \epsilon_0^2 r^4) \left[\frac{3}{4}k_0^2 M^2 - \frac{3k_0 k_1 M \left(\frac{Q}{R}\right)^2}{r} \right] z^2 \tag{3.3}$$

$$\dot{x} = \frac{Q}{8\pi\epsilon_0 r^2} yx - \frac{qQ(32\mu_0\pi^2 \epsilon_0^2 r^4)^2}{4\pi\epsilon_0 r^2 (kQ^2)^2} \left[\left(\frac{3}{4}k_0^2 M^2\right)^2 - \left(\frac{3k_0 k_1 M \left(\frac{Q}{R}\right)^2}{r}\right)^2 \right] y \tag{3.4}$$

where, $\dot{\theta} = z ; \dot{r} = y ; \dot{t} = x$

4. DYNAMICAL SYSTEM AND PHASE SPACE ANALYSIS OF THE GEODESICS:

In this section we will look at the different cases of stability analysis by changing r, k_0, k_1 of the system and we identified the critical points where the system reaches equilibrium and analysed the phase space diagrams. The stability analysis was performed by evaluating the eigenvalues of the Jacobian matrix at each critical points. The presence of eigenvalues with negative real parts indicated stable equilibrium points, while eigenvalues with positive real parts indicated unstable equilibrium points. Complex eigenvalues suggested oscillatory behaviour [11].

We will compute the critical points for a galactic supermassive black hole with mass of $4 \times 10^6 M_\odot$ and the charge by mass ratio of a charged blackhole is taken to be approximately 100 Coulombs per Solar mass [9] and the angular momentum for a reissner blackhole taken to be zero even though the angular velocity is around 0.48 as given in [10]. Therefore the charge of this blackhole becomes 4×10^8 coulombs. Here in this case the charge by mass ratio will be always greater than 1 and if it’s less than 1 then we need to consider negligible charge.

For computing the radius of the charged blackhole;

$$R = \frac{GM}{c^2} + \sqrt{\left(\frac{GM}{c^2}\right)^2 - \left(\frac{Q^2}{Gc^4}\right)^2} \quad (4.1)$$

We got R as $5.927 \times 10^{12} \text{m}$ for this case. We will consider four cases of changing r, k_0 and k_1 as in this model we assumed that $k_0, k_1 \ll r$.

Far from Horizon:

The critical points for $r=10^{20}$, $k_0=10^8$, $k_1=10^5$, $M=4 \times 10^6 M_\odot$, $Q=4 \times 10^8 \text{ C}$, $R=5.927 \times 10^{12} \text{ m}$, $q=10^3 \text{ C}$ are [1, 1, 1].

Eigenvalues:

$[-9.100168550108147\text{e}+284, -5.477800218385041\text{e}+249, -1.6672496190120494\text{e}+245]$

Jacobian matrix: $[[-9.10016855\text{e}+284, -9.10016855\text{e}+284, -9.10016855\text{e}+284]$

$[2.47071131\text{e}+265, 2.47071131\text{e}+265, 2.47071131\text{e}+265]$

$[-7.53056674\text{e}+260, -7.53056674\text{e}+260, -7.53056674\text{e}+260]]$

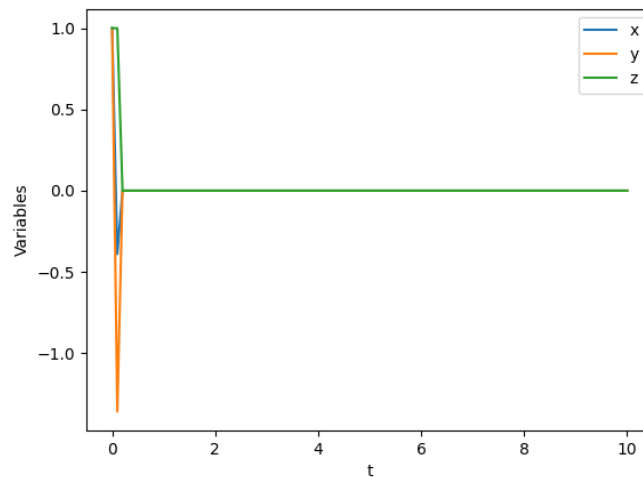


Fig 1: All the variable were chaotic at beginning and then it became stable at very large r

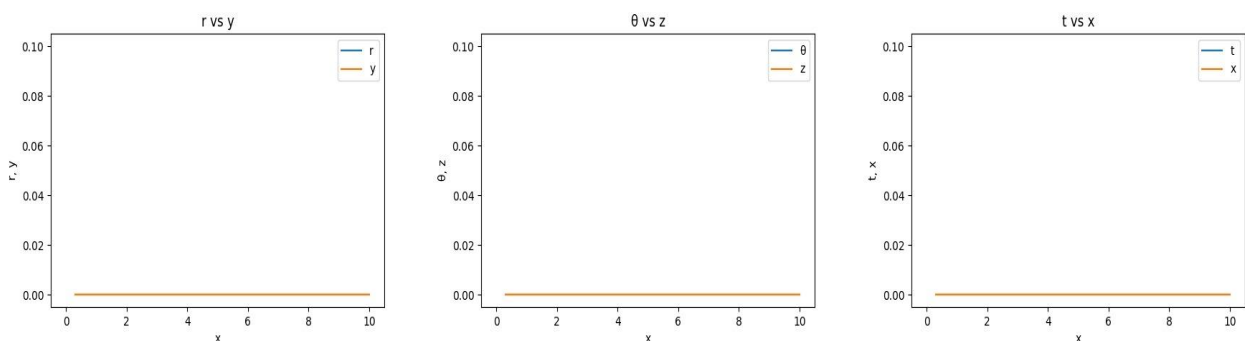


Fig 1.1: In Phase space diagram of Fig 1 there is no potential divergence in the graph so it indicates stability

The eigenvalues are highly negative with large exponential values which suggests high stability of the system at a very large r.

At Horizon:

The critical points for $r=10^{12}$, $k_0=100$, $k_1=90$, $M=4 \times 10^6 M_\odot$, $Q=4 \times 10^8 \text{ C}$, $R=5.927 \times 10^{12} \text{ m}$, $q=10^3 \text{ C}$ are $[-1.19201108\text{e}-69, 8.95269362\text{e}-91, 1.00000000\text{e}+00]$.

Eigenvalues: [0.0, 2.4707558688213548e+265, 1.1344949965674093e+225]

Jacobian matrix: [[4.45555931e+260, 4.45555931e+260, 4.45555931e+260]
 [2.47071131e+265, 2.47071131e+265, 2.47071131e+265]
 [2.54100349e+241, 2.54100349e+241, 2.54100349e+241]]

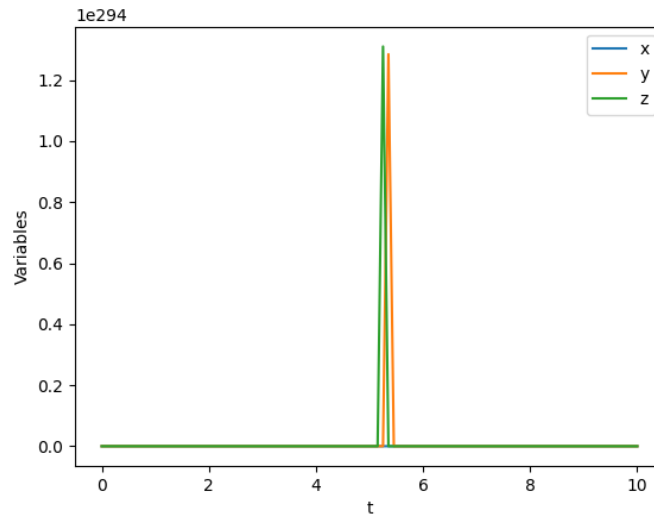


Fig 2: At the horizon the system comes to the critical stability showed by ‘x’ whereas the other variables showed high instability

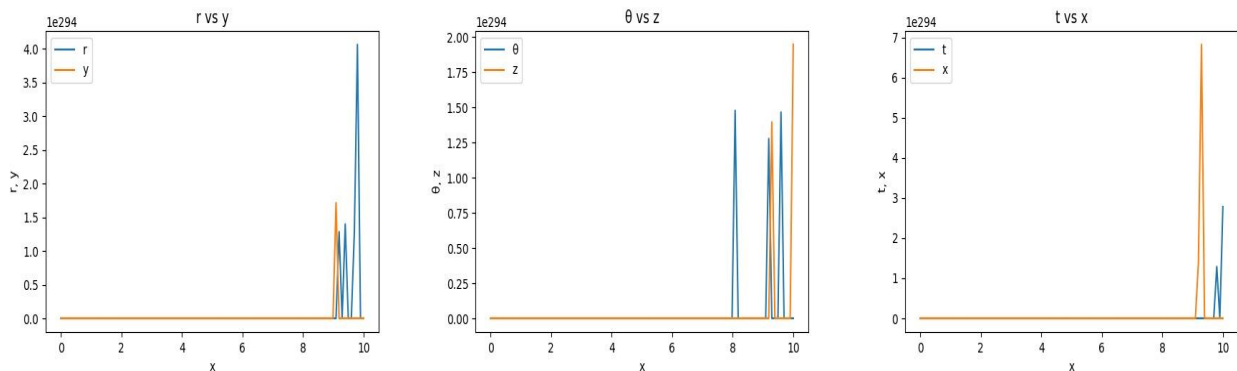


Fig 2.1: In the Phase space diagram of Fig 2, at the beginning it was critically unstable and gradually it diverges suggesting unstable state

The last two eigenvalues have highly positive values showing instability whereas the first eigenvalue showed the critical stability due to zero eigenvalue, which means the system at the horizon is not fully unstable but on the verge of instability.

Near Horizon:

The critical points for $r=10^5$, $k_0=10$, $k_1=5$, $M=4 \times 10^6 M_\odot$, $Q=4 \times 10^8 C$, $R=5.927 \times 10^{12} m$, $q=10^3 C$ are $[-1.19201108e-61, -2.05588159e-82, 1.00000000e+00]$.

Eigenvalues: [4.455507965717163e+260, 3.599130618579141e+233, 1.6089368130980707e+226]

Jacobian matrix: [[4.45550797e+260 , 4.45550797e+260 , 4.45550797e+260]
 [-1.33360294e+249, -1.33360294e+249, -1.33360294e+249]
 [2.54100349e+241, 2.54100349e+241, 2.54100349e+241]]

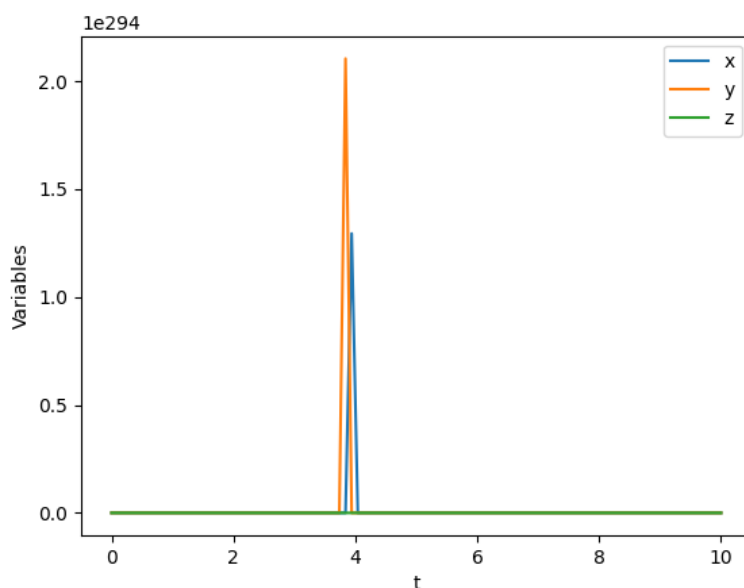


Fig 3: The variables are all very unstable due to highly positive values and as time passes it will be more chaotic and unpredictable

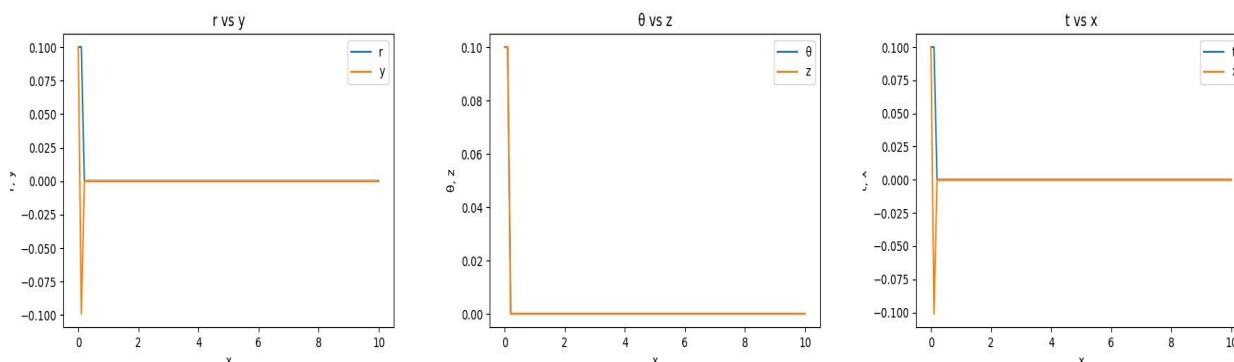


Fig 3.1: In the Phase space diagram of Fig 3, the system is very unstable and chaotic at beginning and it converges suggesting the contracting behaviour

The eigenvalues are very highly positive and shows the high instability in the system as the r goes inside the horizon.

Near Singularity:

The critical points for $r=10^{-30}$, $k_0=10^{-40}$, $k_1=10^{-60}$, $M=4 \times 10^6 M_\odot$, $Q=4 \times 10^8 C$, $R=5.927 \times 10^{12} m$, $q=10^3 C$ are $[2.51369975e-132, 2.66211189e-115, 3.05122660e-115]$.

Eigenvalues:

$9.100168550108147e+284+0j, (1.4826166954317395e+248+1.778524442542522e+254j),$
 $(1.4826166954317395e+248-1.778524442542522e+254j)]$

Jacobian matrix: $[[-9.10016855e+284, -9.10016855e+284, -9.10016855e+284]$

$[9.88284525e+263, 9.88284525e+263, 4.94142262e+263]$

$[-7.53056674e+260, -7.53056674e+260, -7.53056674e+260]]$

[(-

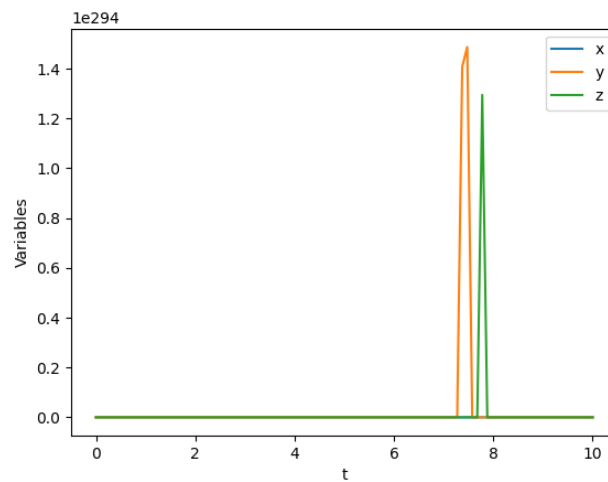


Fig 4: The variables are highly unstable with complex numerical values which represents oscillatory behaviour in the trajectories at it reaches the singularity and the system becomes more complex in nature

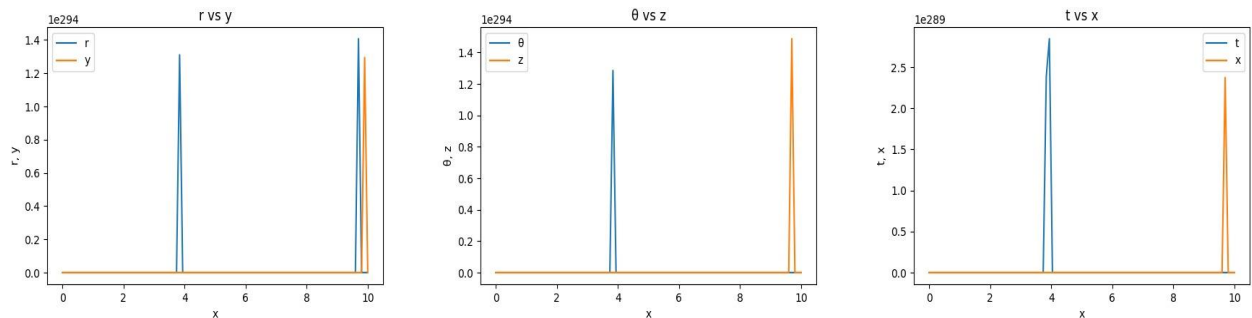


Fig 4.1: In the Phase space diagram of Fig 4, there are instability in the system and the peaks are diverging which indicates expanding behaviour

The complex eigenvalues contributes to a highly unstable system with oscillatory projections and the negative eigenvalues gives a little bit of stability to the system making it more complicated and unpredictable as r approaches near singularity.

Summarized TABLE:

| Case | r (m) | k_0 | k_1 | Critical points | Eigenvalues | Stability analysis |
|------------------|------------|------------|------------|--|--|---|
| Far from Horizon | 10^{20} | 10^8 | 10^5 | [1, 1, 1] | [-9.100168550108147e+284, 5.477800218385041e+249, 1.6672496190120494e+245] | - Very stable |
| At Horizon | 10^{12} | 100 | 90 | [-1.19201108e-69 , 8.95269362e-91 , 1.00000000e+00] | [0.0, 2.4707558688213548e+265, 1.1344949965674093e+225] | Critically stable |
| Near Horizon | 10^5 | 10 | 5 | [-1.19201108e-61 , -2.05588159e-82 , 1.00000000e+00] | [4.455507965717163e+260, 3.599130618579141e+233, 1.6089368130980707e+226] | Very unstable |
| Near Singularity | 10^{-30} | 10^{-40} | 10^{-60} | [2.51369975e-132, 2.66211189e-115, 3.05122660e-115] | [(-9.100168550108147e+284+0j), (1.4826166954317395e+248 +1.778524442542522e+254j), (1.4826166954317395e+248 -1.778524442542522e+254j)] | Highly complex system with more instability |

Now we will take three cases of different test charge and keep r , k_0 and k_1 as constant.

$q = 0$ ($q < Q$):

The critical points for $r=10^5$, $k_0=10$, $k_1=5$, $M=4 \times 10^6 M \odot$, $Q=4 \times 10^8 C$, $R=5.927 \times 10^{12} m$, $q=0 C$ are $[-1.36531465e-120, -1.93225462e-121, -2.38129412e-147]$.

Eigenvalues:

$[4.9415117392496734e+263, 8.910855234581177e+258, 4.1811629740746546e+225]$

Jacobian matrix: $[[1.78221345e+259, 8.91111861e+258, 8.91111861e+258]$

$[4.94142263e+263, 4.94142263e+263, 4.94142263e+263]$

$[1.01640140e+240, 5.08200699e+239, 5.08200699e+239]]$

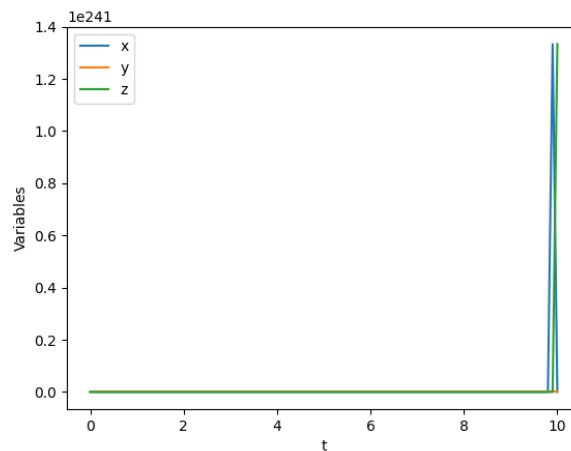


Fig 5: The system becomes very unstable as time passes as the test charge is zero it has very minimal effect in the system

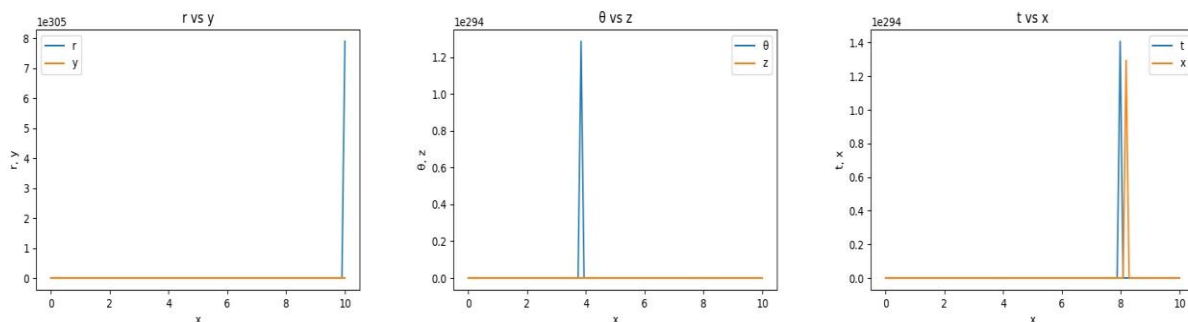


Fig 5.1: In the Phase space diagram of Fig 5, the system diverges more in these graphs suggesting that it's shifting towards more instability

The eigenvalues of the system are very positive with high exponentials representing a very unstable system.

$q > Q$:

The critical points for $r=10^5$, $k_0=10$, $k_1=5$, $M=4 \times 10^6 M \odot$, $Q=4 \times 10^8 C$, $R=5.927 \times 10^{12} m$, $q=10^{30} C$ are $[-1.19201107e-088, -2.16953014e-109, 9.99999998e-001]$.

Eigenvalues: $[0.0, 0.0, 4.455507965730499e+260]$

Jacobian matrix: $[[4.45550797e+260, 3.00667220e-146, 2.54100349e+241]$

$[4.45550797e+260, 3.00667220e-146, 2.54100349e+241]$

$[4.45550797e+260, 3.00667220e-146, 2.54100349e+241]]$

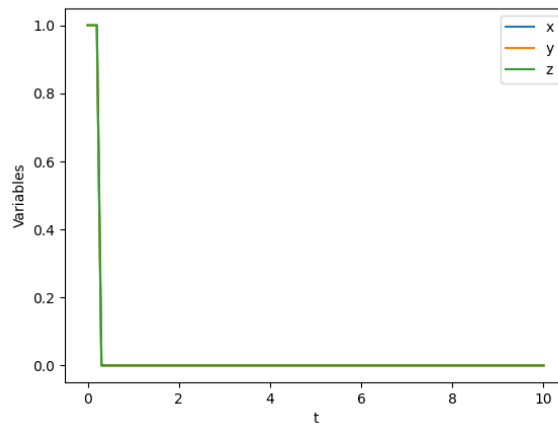


Fig 6: The system very unstable at the beginning and drastically changes to critically unstable state

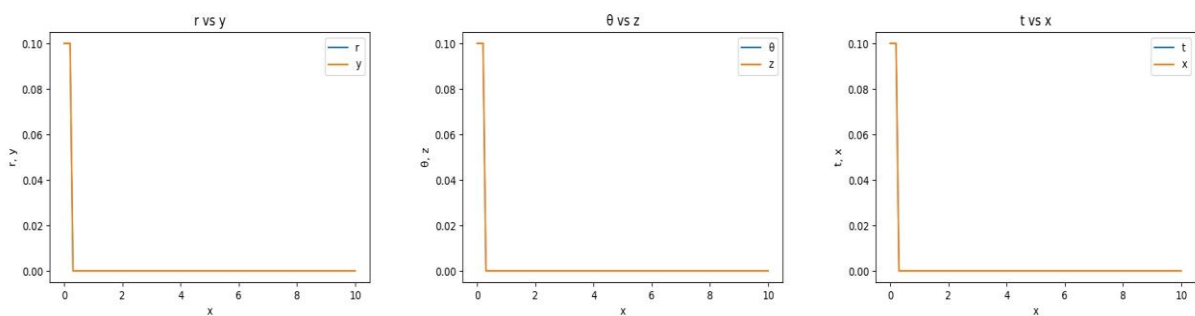


Fig 6.1:In the Phase space diagram of Fig 6, The chaotic system converges and becomes critically unstable

As the two eigenvalues are zero so they makes the system critically unstable but in the same time the high positive eigenvalues makes it very unstable and the high test charge affects the blackhole’s structure and potential.

$$q = Q:$$

The critical points for $r=10^5$, $k_0=10$, $k_1=5$, $M=4 \times 10^6 M_\odot$, $Q=4 \times 10^8 C$, $R=5.927 \times 10^{12} m$, $q = 4 \times 10^8 C$ are $[-2.98002767e-67, 5.75284390e-93, 9.99999996e-01]$.

Eigenvalues: $[0.0, 2.0260278323478486e+265, 6.1975694962367765e+239]$

Jacobian matrix: $[[4.45555007e+260, 4.45555007e+260, 4.45554904e+260]$

$[2.02598328e+265, 2.02598328e+265, 1.97656905e+265]$

$[2.54100349e+241, 2.54100349e+241, 2.54100349e+241]]$

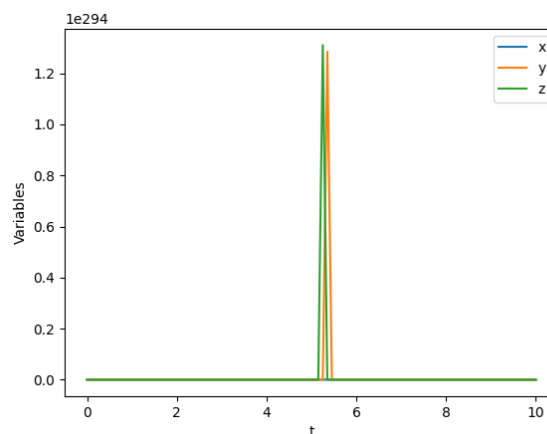


Fig 7: The system is totally on the verge of being critically unstable at beginning and then shifts to being unstable

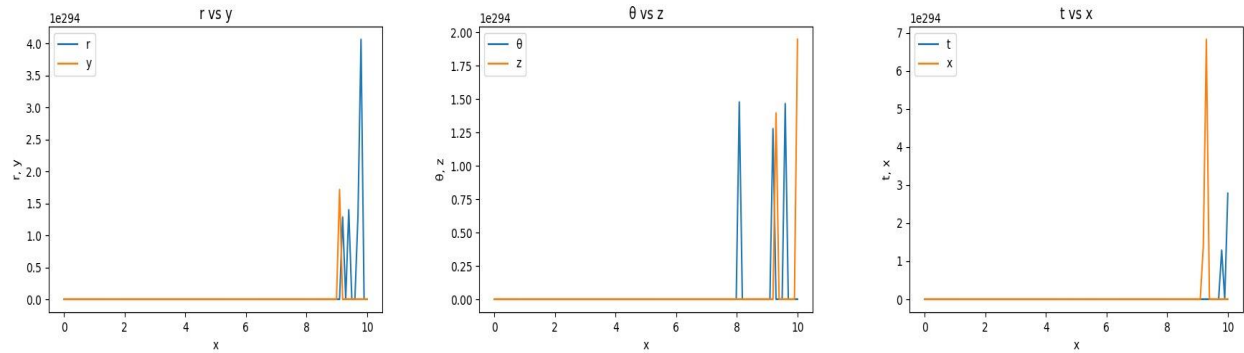


Fig 7.1:In the Phase space diagram of Fig 7, the system was critically unstable and as the peaks diverges more the unstable state expands

The zero eigenvalue contributes to the state of critically unstable and then apparently as the eigenvalue becomes very positive with high exponentials then it becomes highly unstable.

Summarised TABLE:

| Case | q (C) | Critical points | Eigenvalues | Stability Analysis |
|------|---------------------|--|--|--|
| q<Q | 0 | [-1.36531465e-120, 1.93225462e-121, 2.38129412e-147] | - [4.9415117392496734e+263, 8.910855234581177e+258, 4.1811629740746546e+225] | Very Unstable |
| q>Q | 10 ³⁰ | [-1.19201107e-088, 2.16953014e-109, 9.99999998e-001] | - [0.0, 0.0, 4.455507965730499e+260] | Unstable at beginning and then shifts to critically unstable state |
| q=Q | 4 × 10 ⁸ | [-2.98002767e-67 5.75284390e-93 9.99999996e-01] | , [0.0, 2.0260278323478486e+265, 6.1975694962367765e+239] | Critically unstable |

5. SPECTRAL EXPANSION

In this section we will focus on the spectral expansion of the coordinate diagrams of the geodesics (3.2), (3.3), (3.4) and analyse the different conditions.

Changing r , k_0 and k_1 :

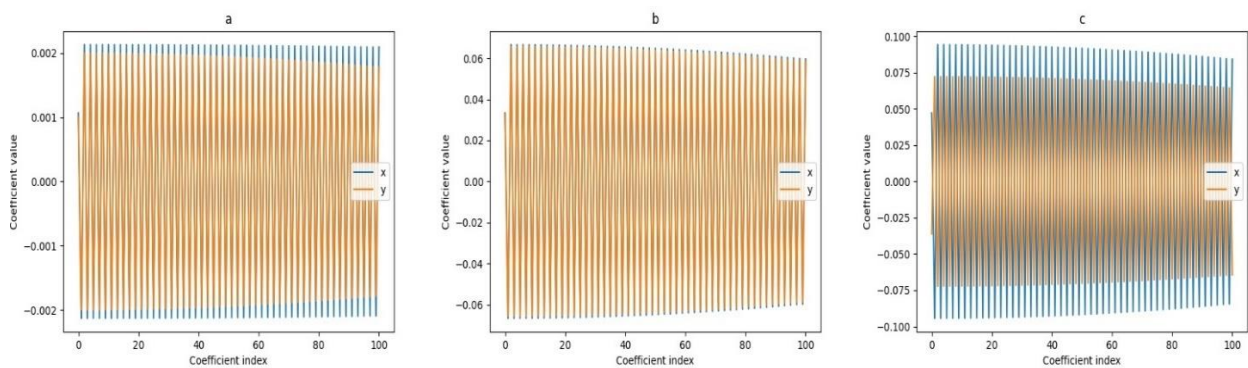


Fig 8: In part (a) when it's far from horizon, the spectral expansion of x effect minimal, in part (b) near the horizon, x effects very less and y becomes dominant, in (c) near the singularity the spectral expansion of x expands and overlaps with y

Changing test charge q :

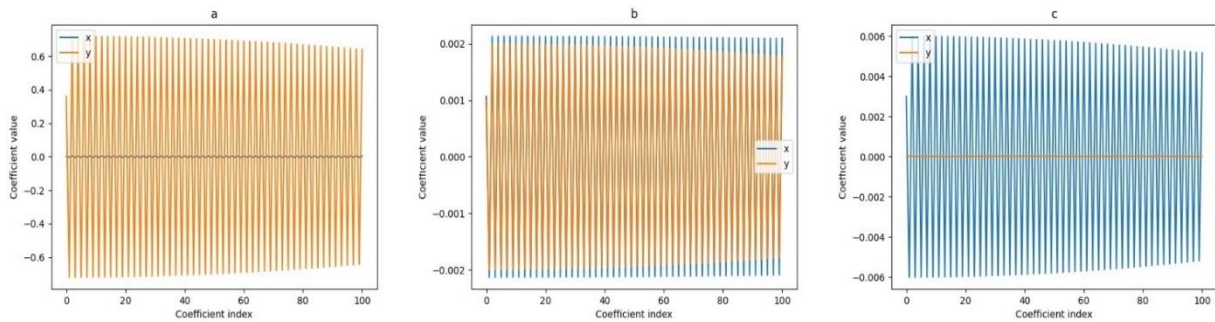


Fig 9: in part (a) $q=0$ and $q < Q$ and y becomes dominant in spectral expansion, in part (b) $q=Q$, x shows minimal spectral expansion, in part (c) $q > Q$, in this case the test charge is very large compared to the charge of black hole so x shows the maximum spectral expansion

6. POINCARÉ TRAJECTORIES

We used the modified metric of Reissner's black hole (2.3.14) and by analysing each components of the metric we computed the Poincaré trajectories of the particles and test charges and we will analyse each conditions of varying R .

Poincaré Projection of the Metric:

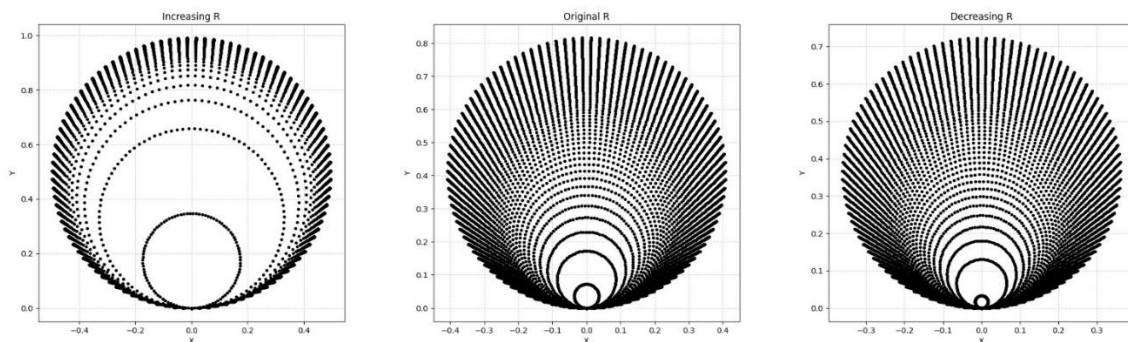


Fig 10: Increasing R in the Poincaré projection increases the singularity and in decreasing the same decreases the singularity of the modified Reissner Nordström black hole in measure

Relation of Coupling constant with changing parameters:

In the previous sections we have looked at the assumptions of λ and ν to be gravitational potential and electromagnetic potential respectively. The vector potential was assumed as $\lambda(r) = A_\mu = \frac{Q}{4\pi\epsilon_0 r}$ (2.3.10) and scalar gauge field as $\nu(r) = V_\mu = \alpha\phi$ (2.3.11), where α is the coupling constant and both λ and ν are functions of r and relations between λ and ν determines the value of α and to analyse the conditions.

We will consider the four cases we took in section 4 with varying r , k_0 , k_1 and will take count of the three cases i) $\lambda > \nu$, ii) $\lambda < \nu$ iii) $\lambda = \nu$.

i) Considering $Q = 4 \cdot 10^8$, $r = 10^20$, $k_0 = 10^8$, $k_1 = 10^5$, $M = 4 \cdot 10^36$, $R = 5.927 \cdot 10^12$ gives $\alpha = 8.987551787368178e - 49$.

a) Condition: $\lambda = \nu$, $\lambda: 0.03595020714947271$, $\nu: \alpha (4e+46)$, $\alpha: 8.987551787368178e-49$

b) Condition: $\lambda > \nu$, $\alpha < 8.987551787368178e-49$

c) Condition: $\lambda < \nu$, $\alpha > 8.987551787368178e-49$

ii) Considering $Q = 4 \cdot 10^8$, $r = 10^12$, $k_0 = 100$, $k_1 = 90$, $M = 4 \cdot 10^36$, $R = 5.927 \cdot 10^12$ gives $\alpha = 8.987551787368178e - 34$.

a) Condition: $\lambda = \nu$, $\lambda: 3595020.714947271$, $\nu: \alpha (4e+39)$, $\alpha: 8.987551787368178e - 34$

b) Condition: $\lambda > \nu, \alpha < 8.987551787368178e - 34$

c) Condition: $\lambda < \nu, \alpha > 8.987551787368178e - 34$

iii) Considering $Q = 4 \cdot 10^8, r = 10^5, k_0 = 10, k_1 = 5, M = 4 \cdot 10^{36}, R = 5.927e+12$ gives $\alpha = 8.987551787368178e - 26$.

a) Condition: $\lambda = \nu, \lambda: 3.5950207149472.71, \nu: \alpha (4e+38), \alpha: 8.987551787368178e - 26$

b) Condition: $\lambda > \nu, \alpha < 8.987551787368178e - 26$

c) Condition: $\lambda < \nu, \alpha > 8.987551787368178e - 26$

iv) Considering $Q = 4 \cdot 10^8, r = 10e-30, k_0 = 10e-40, k_1 = 10e-60, M = 4 \cdot 10^{36}, R = 5.927e+12$ gives $\alpha = 8.987551787368179e + 49$.

a) Condition: $\lambda = \nu, \lambda: 3.595020714947271e+48, \nu: \alpha (0.039999999999999994), \alpha: 8.987551787368179e + 49$

b) Condition: $\lambda > \nu, \alpha < 8.987551787368179e + 49$

c) Condition: $\lambda < \nu, \alpha > 8.987551787368179e + 49$

Summarised TABLE:

| Case | r (m) | k_0 | k_1 | Coupling constant (α) |
|----------------------|------------|------------|------------|--------------------------------|
| Far from horizon | 10^{20} | 10^8 | 10^5 | $8.987551787368178e - 49$ |
| At horizon | 10^{12} | 100 | 90 | $8.987551787368178e - 34$ |
| Near horizon | 10^5 | 10 | 5 | $8.987551787368178e - 26$ |
| Near the singularity | 10^{-30} | 10^{-40} | 10^{-60} | $8.987551787368179e + 49$ |

From these four conditions, it's observed that when gravitational potential is more than electromagnetic potential then coupling constant is very less and vice-versa, and secondly when the distance r was large means when it's far from horizon α was very less and gradually increased we move towards the singularity and in the last case the coupling constant α suddenly jumped to a very higher value with a large exponential suggesting the coupling between gravitational potential and electromagnetic potential is very high near the singularity.

Now last but not least we will show the visual representation of Coupling between Scalar Gauge Field and Gravitational Potential with varying charge of the blackhole Q taking the coupling constant α fixed.

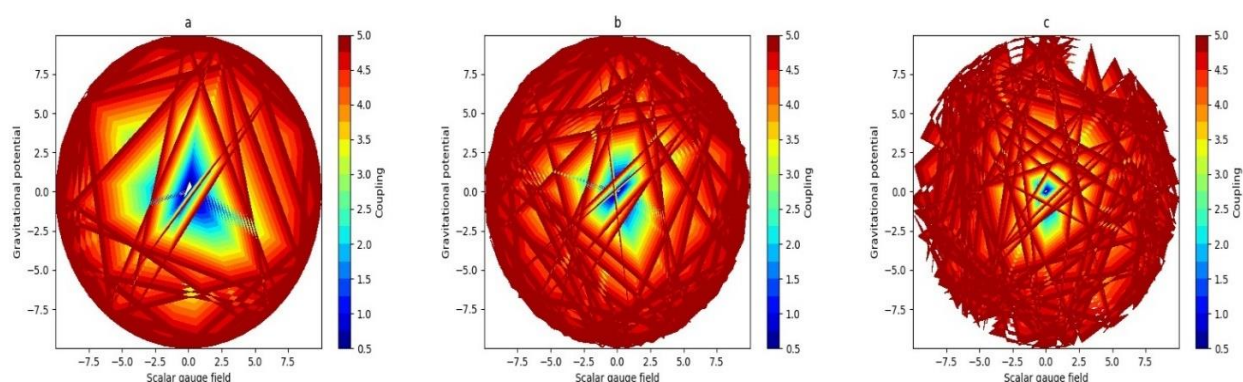


Fig 11: Coupling between Scalar Gauge Field and Gravitational Potential; in part (a) with decreasing Q the coupling between scalar field and gravitational field has also decreased and in part (b) the coupling increased gradually and in part (c) it increased abruptly.

Therefore in this section we have looked at how the coupling constant goes to infinity as r becomes zero and vice-versa and they are inversely proportional in addition we also visualised the situation in the Fig 11 by the graph between the scalar gauge field and the vector field.

7. RESULT

From the observations of these previous sections we have computed the stability analysis for each of the conditions through determining their eigenvalues and with phase space analysis. We have also looked into the spectral expansion of various conditions and the Poincaré Projection of the metric. Finally we showed the variation of the coupling constant with changing r , k_0 , k_1 and the diagram of varying coupling constant between gravitational potential and scalar gauge potential.

8. CONCLUSION

In this study, we have investigated the modified Reissner-Nordström metric in Lyra's geometry by computing the modified field equations and obtaining expressions for e^λ and e^ν . Through these calculations, we aimed to understand the implications of Lyra's geometry on the gravitational field of a charged black hole.

Furthermore, we conducted stability analysis to examine the stability of the system and phase space analysis to gain insights into the dynamical behaviour of the geodesics. These analyses provided valuable information about the stability and qualitative characteristics of the system. Additionally, we explored the spectral expansion under various conditions, which allowed us to analyse the behaviour of the metric in different regimes. Moreover, we employed the Poincaré projection to visualize the spacetime geometry of the black hole and understand its properties.

ACKNOWLEDGEMENT

I would like to express my sincere gratitude towards Prof. Biswajit Paul whose work has contributed to my understanding of principles of Reissner black hole and the dynamical system analysis and various other techniques and Prof. Subrata Bhowmik who contributed to the understandings of the Lyra's geometry and its applications. I am thankful to both of the professors to shape my knowledge of Lyra's geometry and Reissner's spacetime and to provide the foundation for this project.

Conflicts of Interest:

There is no conflict of interest to declare regarding this project.

REFERENCES

- [1]. W.D. Halford, "Cosmological Theory Based on Lyra's Geometry." April 20, 1970 <https://www.semanticscholar.org/paper/COSMOLOGICAL-THEORY-BASED-ON-LYRA'S-GEOMETRY.-Halford/acee750c8aa82aa784917b7eefcbccd8682d158e>.
- [2]. F. Rahaman, A. Ghosh, and M. Kalam, "Lyra Black Holes." "[gr-qc/0612042] Lyra black holes - arXiv.org." 07 Dec. 2006, <https://arxiv.org/abs/gr-qc/0612042>.
- [3]. R.R. Cuzinatto, E.M. de Moraes, and B.M. Pimentel, PHYSICAL REVIEW D103,124002 (2021) "Lyra Scalar-Tensor Theory: A Scalar-Tensor Theory of Gravity on Lyra Manifold." 13 Apr. 2021, DOI: 10.1103/PhysRevD.103.124002
- [4]. D.K. Sen, "On geodesics of a modified Riemannian manifold", Can. Math. Bull, **3**, (1960) 255
- [5]. R.R. Cuzinatto, E.M. de Moraes, and B.M. Pimentel, "LyST: A Scalar-Tensor Theory of Gravity on Lyra Manifold." 13 Apr. 2021, <https://arxiv.org/abs/2104.06295v1>.
- [6]. Jonatan Nordebo, "The Reissner-Nordström Metric" Semantic Scholar. <https://www.semanticscholar.org/paper/The-Reissner-Nordstr%C3%B6m-metric-Nordebo/9311976210064b18e4f59223665cdb14cffb6c26/figure/0>.
- [7]. Ramesh Tikekar, "A Source for the Reissner-Nordström Metric" Journal of Astrophysics and Astronomy· September 1984, DOI: 10.1007/BF0271454 <https://link.springer.com/article/10.1007/BF02714543>.
- [8]. D.K. Sen "A static cosmological model", Zeit. f. Physik **149**, (1957), 311
- [9]. "Charged black holes in GR and beyond" by N. K. Johnson-McDaniel Benasque meeting 04.06.2018 https://www.benasque.org/2018relativity/talks_contr/049_McDaniel.pdf.
- [10]. "Electric charge of black holes: Is it really always negligible?" By Michal Zajacek1 and Arman Tursunov2 09 Apr. 2019, <https://arxiv.org/abs/1904.04654>.
- [11]. PHYSICAL REVIEW D95,124060 (2017) "Dynamical analysis of an integrable cubic Galileon cosmological model" Alex Giacomini, Sameerah Jamal, Genly Leon, Andronikos Paliathanasis, and Joel Saavedra, DOI:10.1103/PhysRevD.95.124060